Title

Brain Volume Change and Cognitive Trajectories in Aging

Journal

Neuropsychology, 32(4)

ISSN

0894-4105

Authors

Fletcher, Evan

Gavett, Brandon

Harvey, Danielle

et al.

Publication Date

2018-05-01

DOI

10.1037/neu0000447

Peer reviewed

Published in final edited form as:

Neuropsychology. 2018 May ; 32(4): 436–449. doi:10.1037/neu0000447.

Brain Volume Change and Cognitive Trajectories in Aging

Evan Fletcher,
Department of Neurology, University of California, Davis

Brandon Gavett,
Department of Psychology, University of Colorado, Colorado Springs

Danielle Harvey,
Department of Public Health Sciences, University of California, Davis

Sarah Tomaszewski Farias,
Department of Neurology, University of California, Davis

John Olichney,
Department of Neurology, University of California, Davis

Laurel Beckett,
Department of Public Health Sciences, University of California, Davis

Charles DeCarli, and
Department of Neurology, University of California, Davis

Dan Mungas
Department of Neurology, University of California, Davis

Abstract

Objective—Examine how longitudinal cognitive trajectories relate to brain baseline measures and change in lobar volumes in a racially/ethnically and cognitively diverse sample of older adults.

Method—Participants were 460 older adults enrolled in a longitudinal aging study. Cognitive outcomes were measures of episodic memory, semantic memory, executive function, and spatial ability derived from the Spanish and English Neuropsychological Assessment Scales (SENAS). Latent variable multilevel modeling of the four cognitive outcomes as parallel longitudinal processes identified intercepts for each outcome and a second order global change factor explaining covariance among the highly correlated slopes. We examined how baseline brain volumes (lobar gray matter, hippocampus, and white matter hyperintensity) and change in brain volumes (lobar gray matter) were associated with cognitive intercepts and global cognitive change. Lobar volumes were dissociated into global and specific components using latent variable methods.

Results—Cognitive change was most strongly associated with brain gray matter volume change, with strong independent effects of global gray matter change and specific temporal lobe gray

Correspondence concerning this article should be addressed to Evan Fletcher, Center for Neuroscience, University of California, Davis, 1544 Newton Court, Davis, CA 95616. evanfletcher@gmail.com.

matter change. Baseline white matter hyperintensity and hippocampal volumes had significant incremental effects on cognitive decline beyond gray matter change. Baseline lobar gray matter was related to cognitive decline, but did not contribute beyond gray matter change.

Conclusion—Cognitive decline was strongly influenced by gray matter volume change and, especially, temporal lobe change. The strong influence of temporal lobe gray matter change on cognitive decline may reflect involvement of temporal lobe structures that are critical for late life cognitive health but also are vulnerable to diseases of aging.

General Scientific Summary

This is a foundational study that rigorously establishes a hierarchy of brain factors associated with cognitive decline. It shows that brain change factors of global brain gray matter atrophy, and incrementally, temporal lobe gray matter atrophy, are the strongest predictors of longitudinal cognitive change. Other significant predictors are baseline hippocampal volume and brain white matter intensity load.

Keywords

aging; cognitive change; gray matter volume; gray matter change; white matter hyperintensity

Cognitive decline in older adults is a major public health problem that has enormous personal, familial, and societal impacts. A large body of research has demonstrated that cognitive decline is not a universal consequence of aging, but rather, with aging comes heterogeneity of cognitive trajectories such that some individuals decline with widely variable ages of onset while others remain cognitively healthy across the older adult age span. Understanding this heterogeneity and the brain mechanisms associated with cognitive decline and cognitive health is critical for delineating the processes of normal or “expected” aging and the deviating trajectories that lead to cognitive impairment and dementia. This has major implications for clinical care of older individuals, and for developing interventions to prevent or reduce the impact of brain diseases on cognitive decline and dementia.

Exploring the relations of aging and disease to brain change, and of brain change to cognition, are key aspects of this pursuit. Although cross-sectional studies have made vital contributions to these questions, longitudinal studies can in principle provide robust measures of brain change trends over time (Raz et al., 2005), avoid certain biases of cross sectional data (Fjell, McEvoy, Holland, Dale, & Walhovd, 2014) and better represent the association of brain factors and cognition than cross-sectional data (Raz & Rodrigue, 2006).

Prevalent approaches to longitudinal quantification have made use of differences in region of interest (ROI) measurements from subsequent images (Mungas et al., 2005a; Raz et al., 2005; Resnick, Pham, Kraut, Zonderman, & Davatzikos, 2003) or registration to a normalized template in order to generate tissue density maps (Driscoll et al., 2009; Resnick et al., 2003), using the so-called “RAVENS” technique (Davatzikos, Genc, Xu, & Resnick, 2001). Another recent approach, which we shall use in this paper, computes longitudinal atrophy rates from nonlinear registration of same-subject structural MRI scans at successive time points. Techniques incorporating deformation maps to quantify local change fall under the umbrella term of tensor-based morphometry (TBM; Ashburner & Friston, 2000; Leow et

al., 2007). Applied to longitudinal scans, they can provide precise voxel-level localization of longitudinal brain change (Christensen, Joshi, & Miller, 1997), but they require careful regularization to avoid introducing biases (Yanovsky, Leow, Lee, Osher, & Thompson, 2009).

Recent studies have used a variant of TBM (Holland & Dale, 2011) to examine local brain atrophy rates related to aging. One study of healthy cognitive aging adults (Fjell et al., 2009) found an average annual decline in temporal and prefrontal cortices of around 0.5% along with significant declines in subcortical and periventricular regions, concluding that normal aging in the absence of identified pathological processes is associated with substantial atrophy in these regions. Another study of atrophy rates in normal older participants with low probability of Alzheimer's disease (AD) pathology (Fjell, McEvoy, Holland, Dale, & Walhovd, 2013) showed losses in fronto-temporal regions and areas overlapping the default mode network (DMN). In their review of current results of the time (Fjell et al., 2014) argued that longitudinal studies support a "normalcy-pathology homology" whereby regions of high plasticity are both vulnerable to normal aging losses (Raz et al., 1997) and susceptible to added AD pathology. In contrast, a survey of atrophy results in normal aging and AD (Pini et al., 2016) stated that atrophy patterns associated with aging are qualitatively and quantitatively different than those associated with disease. However, they also described an incipient AD stereotypical pattern of cortical loss recapitulating the Braak stages of NFT pathology, suggesting that at least at the earliest stages, there is a convergence of AD-related atrophy and brain changes related to healthy cognitive aging.

These studies point to the need for further work to clarify different fundamental hypotheses of brain atrophy trajectories: (a) qualitatively similar pathways for brain changes in healthy and pathological aging but quantitatively greater inputs to these pathways in disease, versus (b) qualitatively different pathways that might also have quantitatively different inputs.

Understanding brain effects on cognition is the second major requirement for a comprehensive explanation of healthy and pathological cognitive aging trajectories. There is an extensive literature examining how brain variables relate to cognition and cognitive decline, but much of this literature is based on cross-sectional associations of brain and cognition, and less commonly, on using cross-sectional brain variables to predict cognitive decline. Studies of cognitive decline that include comprehensive brain measures are limited, and studies that examine effects of brain changes are especially limited. Comprehensive, multiple domain measurement of cognition also is relatively uncommon, as is use of cognitive outcome measures that are optimized for measuring longitudinal change. Consequently, there have been comparatively few studies focused on the interrelationships between baseline brain characteristics, longitudinal brain change and longitudinal cognitive change.

A review of extant literature at that time (Raz & Rodrigue, 2006) noted modest associations between cross-sectional brain volumes and cognitive performance, but suggested that brain atrophy rates showed more significant associations with cognition than did cross-sectional measurements. For example, (Rodrigue & Raz, 2004) showed that after controlling for age, only the annual rate of shrinkage in the entorhinal cortex (ERC) predicted poorer memory.

There have been other reports of effects of brain change on cognition. A study of both baseline and longitudinal volume change effects (Mungas et al., 2005a) reported that memory change was related both to baseline and change measures in the hippocampus, whereas executive function change was associated with baseline gray matter (GM) and longitudinal GM change, hippocampal change and the incidence of lacunes. TBM studies have also found associations between brain changes and cognition. Murphy et al. (2010) showed that 6-month temporal lobe region atrophy rates correlated with subsequent memory loss. McDonald et al. (2012) found atrophy differences between mild cognitively impaired (MCI) and normal participants, and further identified, among MCI, differing regional atrophy associations with declines in specific cognitive domains.

Previous TBM studies have demonstrated potential for identifying associations of localized progression of atrophy with specific cognitive changes. But TBM has not been widely used in combination with sophisticated measurement and statistical modeling to rigorously test the brain bases of cognitive change. Our study was designed to clarify associations of baseline volumes and longitudinal atrophy rates with cognitive change in four domains. We used baseline brain measurements and TBM calculations of global and regional atrophy along with baseline global white matter hyperintensity to explain change in cognition across multiple domains. Our cognitive outcomes were psychometrically matched measures of episodic and semantic memory, spatial skills, and executive function that have been optimized for tracking longitudinal change in demographically and cognitively diverse older adults (Crane et al., 2008; Mungas et al., 2010; Mungas, Reed, Haan, & Gonzalez, 2005b; Mungas, Reed, Crane, Haan, & González, 2004). We used latent variable modeling to characterize patterns of correlated cognitive trajectories among the four outcomes and to decompose brain GM baseline volumes and atrophy into global and specific components. Our primary hypothesis was that cognitive decline would be best explained by brain volume change. We also examined differential associations of global and specific brain regions on domain specific cognitive decline. A novel aspect of this study was that we not only used psychometrically matched cognitive outcome measures, but also formally evaluated patterns of correlation of change in these measures as well as global and specific brain contribution to this change. This study was intended to fill a gap in the literature on relative contribution of baseline brain and brain change measures to cognitive decline. This is an important step for understanding the broader problem of normal and pathological cognitive aging.

Method

Participants

The University of California, Davis, (UC Davis) Aging Diversity Cohort provided the study sample. This is a longitudinal study of cognitive aging in an educationally, ethnically, and cognitively diverse cohort of older adults. This cohort approximates the diverse racial, ethnic, and socioeconomic composition of a six-county catchment area in the central Sacramento/San Joaquin valley and east San Francisco Bay area of Northern California, is composed of Hispanics, African Americans, and non-Hispanic Whites, has wide variability in educational attainment, and spans a spectrum of cognitive function from normal to mildly impaired to demented. Cohort composition and recruitment methods are described in

(Hinton et al., 2010). Participants were 460 persons who had received at least two cognitive evaluations and at least one MRI brain scan; 295 had two or more scans. There were 212 Caucasians, 111 Hispanics, and 121 African Americans and 16 other races/ethnicities; 64 Hispanics were tested in Spanish, and all others were tested in English. A community screening program designed to identify and recruit individuals with cognitive functioning representative of the community dwelling population identified 313 individuals (97 Caucasians, 98 Hispanics, 107 African Americans, 11 other). The remaining 147 (115 Caucasians, 13 Hispanics, 14 African Americans, 5 other) were initially seen for clinical evaluation at a university memory/dementia clinic and referred for research.

Participants were evaluated and followed within the research program of the University of California at Davis Alzheimer's Disease Center (UCD ADC). Enrollment began in 2001 and a rolling enrollment design was used to build the cohort with substantial enrollment continuing through 2010. All participants in this study had at least two evaluations but due to rolling enrollment there was variability in the number of evaluations completed by each participant. Inclusion criteria for the longitudinal cohort included age 60 or older at their first examination and ability to speak English or Spanish. Exclusion criteria included unstable major medical illness that could have marked effects on cognitive function, major primary psychiatric disorder, and substance abuse or dependence in the last five years. Examples of unstable major medical illnesses that would be excluded include heart failure, cancer with active chemotherapy, and severe respiratory disease. Chronic diseases like hypertension and diabetes were not excluded even if not under medical control. Participants received clinical evaluations through the UCD ADC on a roughly annual basis that included diagnosis, based on standard diagnostic criteria, of normal cognition versus mild cognitive impairment (MCI) versus dementia as well as etiologic diagnosis. All participants signed informed consent, and all human subject involvement was overseen by institutional review boards at University of California at Davis, the Department of Veterans Affairs Northern California Health Care System and San Joaquin General Hospital in Stockton, California.

Demographic and clinical characteristics of the sample are presented in Table 1. About 59% were females. Gender differed across diagnosis groups, $\chi^2(2) = 11.356$, $p = .003$; normals and demented cases were more likely to be female but MCI cases were evenly divided among males and females. About 26% were African Americans, 24% were Hispanics, 46% were Caucasians, and 3% were other ethnicities. Ethnicity differed by diagnosis, $\chi^2(6) = 41.050$, $p = .001$ with Whites more likely to have a diagnosis of MCI. Approximately two thirds of the sample was recruited from the community (68%). Recruitment source differed by diagnosis, $\chi^2(2) = 70.848$, $p = .001$, with MCI cases more likely to be clinic referrals. Average age was about 75 years, and this differed across groups, $F(2, 451) = 9.110$, $p = .001$ with demented older than MCI who were older than normals. Average education was 12.9 years and differed across groups, $F(2, 451) = 6.256$, $p = .002$, with highest education in MCI, lowest in demented, and normals in between. Apolipoprotein E (APOE) e4 differed by diagnosis, $\chi^2(2) = 23.231$, $p = .001$ with highest e4 prevalence in demented cases (61%) and lowest in normals (30%). APOE e24 ($N = 16$, 4% of sample) and e44 ($N = 17$, 4%) accounted for relatively small percentages of the overall sample. Hypertension (66% of sample) and hypercholesterolemia (53%) did not differ across diagnosis groups, but diabetes (28%) did differ by diagnosis, $\chi^2(2) = 8.459$, $p = .015$, with highest prevalence in normals.

Cognitive Assessment

The cognitive outcomes in this study were composite measures of episodic memory, semantic memory, executive function, and spatial ability derived from the Spanish and English Neuropsychological Assessment Scales (SENAS). The SENAS has undergone extensive development as a battery of cognitive tests relevant to cognitive aging that allow for valid comparisons across race/ethnic groups (Mungas et al., 2005b, 2004; Mungas, Reed, Marshall, & González, 2000; Mungas, Reed, Tomaszewski Farias, & DeCarli, 2005; Mungas, Widaman, Reed, & Tomaszewski Farias, 2011). Item response theory and confirmatory factor analysis methods were used to evaluate reliability across a broad range of ability relevant to older adults and incorporate items that effectively measure over this ability continuum. This development process yielded composite measures that are psychometrically matched across domains in terms of level of reliability across the ability continuum. It is important to note that these composite scores do not have floor and ceiling effect and are normally distributed. The episodic memory composite score is derived from a multitrial word-list-learning test (Mungas et al., 2004). The semantic memory composite is derived from highly correlated verbal (object-naming) and nonverbal (picture association) tasks. The executive function composite is constructed from component tasks of category fluency, phonemic (letter) fluency, and working memory (digit-span backward, visual-span backward, list sorting). Spatial ability was measured using the SENAS Spatial Localization scale which assess ability to perceive and reproduce two-dimensional spatial relationships that are increasingly complex. These measures were administered at all evaluations. Language of test administration was determined by an algorithm that combined information regarding each participant's language preference in several specific contexts (e.g., conversing at home, listening to radio or TV, conversing outside the home, preferred language for reading). Administration procedures, measure development and psychometric characteristics of the SENAS battery are described in more detail elsewhere (Mungas et al., 2004).

MRI Measures

Baseline volumes (cross-sectional)—MRI baseline measurements were made as part of our in-house processing pipeline described previously (e.g., Fletcher, 2014; Lee et al., 2010). Briefly, structural MRI images were processed to remove the skull using an atlas-based method (Aljabar, Heckemann, Hammers, Hajnal, & Rueckert, 2009) followed by human quality control to provide generally minor cleanup if needed. Structural MRI brain images were then nonlinearly registered to a minimal deformation template (MDT) synthetic brain image (Kochunov et al., 2001) adapted for age range of 60 and above; the registration was performed by a cubic B-spline deformation (Rueckert, Aljabar, Heckemann, Hajnal, & Hammers, 2006). Gray, white and CSF tissues segmentation was initiated automatically by reverse transforming the MDT segmentation onto native structural MRIs using the computed registration parameters. This was the start of an iterative maximal likelihood estimation of tissue classes based upon alternating voxel class assignment followed by tissue class parameter estimation until convergence. The class likelihood priors included terms designed to enhance accuracy at likely tissue boundaries (Fletcher, Singh, Harvey, Carmichael, &

DeCarli, 2012). Finally, native lobar GM volumes were computed by reverse transforming MDT lobar ROIs into native space using the B-spline registration parameters.

Volume change (longitudinal)—For participants having at least two longitudinal structural MRI scan acquisitions, we computed longitudinal structural change between the most widely separated time points. We used a TBM method designed to enhance sensitivity and specificity for biological change by incorporating estimates of likely tissue boundaries (Fletcher, 2014; Fletcher et al., 2013). This processing was done via an in-house processing pipeline that has been previously described (Fletcher et al., 2016). Briefly, we linearly aligned images at Time 1 and Time 2 to a "halfway space" in order to avoid interpolation biases when only one image is transformed. Each brain scan was then corrected for field inhomogeneities using an atlas-based technique and finally tissue-segmented using an algorithm sensitive to edge presence. The log-transformed determinant of the 3 × 3 Jacobian matrix of the TBM deformation at each voxel (i.e., log-Jacobian) quantifies local brain change.

To perform voxel-wise longitudinal change analysis across subjects in a common space, we transformed subject native-space log-Jacobian images onto a minimal deformation (MDT) template space (Kochunov et al., 2001) adapted to an older age-group population. These transformations were generated by affine alignment of native subject structural MRI to MDT, followed by nonlinear B-spline warping (Rueckert et al., 2006), with each subject's alignment and warping deformations then applied to the subject log-Jacobian image. For statistical analysis of longitudinal change in native space, we registered regions of interest (ROIs) to individual participant native space images using backward transformations from MDT as previously described (Lee et al., 2010) and then calculated the mean log-Jacobian value over each ROI segmented for GM. The lobar ROIs used in our analyses were defined in MDT space by an experienced neurologist and have been used in a prior publication from our laboratory (Lee et al., 2010).

APOE genotyping—APOE genotyping was carried out using the LightCycler ApoE mutation detection kit (Roche Diagnostics, Indianapolis, Indiana).

Data Analysis

Measures and data processing—SENAS measures of Episodic Memory, Semantic Memory, Executive Function, and Spatial Ability were the primary dependent variables. Baseline lobar MRI volumes and change in these volumes were the primary independent variables (prefrontal, temporal, parietal minus postcentral gyrus, occipital). Cognitive and baseline MRI variables were reasonably normally distributed. MRI change variable were symmetrical but had high kurtosis. The Blom inverse normal rank order transformation was applied to all cognitive and MRI variables to establish a common scale ($M = 0$, $SD = 1$) and normalize the variables. Age (centered at 70) and education (centered at 12) were continuous covariates. Gender, ethnicity, language of test administration and APOE ε4 status were categorical covariates with female, Caucasian, English test administration and APOE e4 negative serving as reference categories.

Analysis of variance (ANOVAs) and the chi-square test were used to compare baseline characteristics of study participants across diagnostic groups. Mixed effects regression analyses were used to estimate parallel process growth models to characterize cognitive trajectories and to assess the impact of covariates and MRI variables on baseline cognitive scores and rate of change.

MRI modeling—MRI measures of brain structure represent the state of the brain at the time of the scan. Brain size in older individuals is influenced both by the maximal brain size attained in early adulthood and by subsequent brain tissue change and atrophy. Maximal brain size is limited by the size of the intracranial vault, which doesn't change with age. Therefore, it is common practice to adjust brain volumes for intracranial volume (ICV). These adjusted volumes are regarded as measures of brain atrophy—the difference between observed brain size and that expected on the basis of the observed ICV. A second important methodological issue is that brain volumes tend to be highly correlated, even after ICV adjustment. This can present problems of colinearity in estimating regression models that include multiple brain variables, and can also make it difficult to separate effects of specific regions of interest from common effects of brain atrophy. We used latent variable methods to (a) adjust baseline volumes for ICV and (b) decompose correlated groups of MRI measures into global components and lobe-specific deviations from the global averages. The decomposition of global and specific brain effects is a latent variable modeling implementation of the multivariate approach recommended by Salthouse (2011) for capturing specific brain effects as well as higher order effects that are shared across specific brain variables. Figure 1 shows a schematic model of this approach.

For baseline, MRI volumes were regressed on ICV and a global factor (brain bl) was fitted using the four regional ROIs as indicators. The ROI-specific residuals were captured as latent variables. ICV and the global volume factor were constrained to be uncorrelated to identify the model and residuals were uncorrelated with ICV and brain bl ("bl" denotes baseline MRI measurement and "ch" denotes change, representing atrophy rate). This process yielded 6 variables for subsequent analyses: ICV, brain bl, four specific lobar volumes not fully predicted as a simple result of ICV or brain bl. The latent variable brain bl is a summary measure of brain volume that represents a weighted average of the four lobar volumes. The specific lobar components are deviations from what would be expected given the global average.

Volume change was measured by using the TBM approach that inputted the first and last scan to derive a measure of change for each voxel, and voxel level results were summarized in lobar ROI volumes. These four lobar ROI change summary measures were indicators for a global change factor (brain ch) and latent variables were used to capture ROI specific change not fully explained by brain ch. This yielded five latent variables that were used as independent variables in subsequent models: brain ch and the four lobe-specific change variables. This approach to decomposing brain baseline and change measures allowed us to examine how global brain volume influenced cognitive outcomes, but also the incremental effects of specific lobes after controlling for global volume.

Longitudinal modeling of cognitive trajectories—Mixed effects, parallel process longitudinal analyses were performed using MPlus version 7.3 multilevel modeling (Muthén & Muthén, 1998–2012). This modeling platform simultaneously estimates Within and Between level parameters. Figure 2 shows a schematic of the basic modeling approach. In the Within part of the model, each of the four cognitive outcomes was regressed on time in study. This generated person-specific intercept and linear slope random effects for each outcome. These random effects were dependent variables in the Between part of the model. Mixed effects models estimate the baseline value and rate of change of outcomes of interest (within model), and also estimate how differences in these components relate to variables of interest (fixed effects) that differ between subjects (e.g., covariates, MRI variables; between model). The inclusion of random effects accounts for individual variation not measured by the variables included in the model. Mixed effects models allow for heterogeneity in the number of assessment time points and in the lags between assessments across persons.

Model building proceeded in steps. Step 1 developed a base model to estimate intercept and slope random effects for all four outcomes, and included a within-subjects term to account for practice effects. This was an unconditional model that did not include covariates or brain variables. For each of the four cognitive outcome measures, a variable coding for previous exposure versus no exposure was created and included as a time-varying fixed effect. The initial model allowed the eight random effects latent variables (intercept and slope random effects for each of the four outcomes) to freely correlate, but we then estimated second order latent variables (one with intercepts as indicators, one with slopes) that explained the correlations among the random effects. This step was taken to determine whether baseline cognition and cognitive change in our sample was best characterized by the four SENAS composite measures of Episodic Memory, Semantic Memory, Executive Function, and Spatial separately, or by second-order latent variables that estimate “global cognition” reflected in covariance among the four SENAS measures. We compared fit of models with 0, 1, and 2 second-order factors using comparative fit indices including the Akaike Information Criterion (AIC; Akaike, 1987), the Bayesian Information Criterion (BIC; Schwarz, 1978), and the Sample Size Adjusted Bayesian Information Criterion (aBIC; Sclove, 1987). These indices differ in the relative weighting of model fit and model parsimony with AIC valuing parsimony the least and BIC the most. Lower values on all indices indicate better model fit.

In Step 2, we added APOE genotype and age, gender, education, language and ethnicity as fixed effect covariates to explain cognition baseline and change. We examined interaction effects involving ethnicity and other covariates in preliminary analyses and retained any significant interactions in subsequent analyses.

In Step 3 we examined univariable effects of baseline MRI volumes and MRI volume change on cognition. First, we added specific MRI baseline volumes one at a time to the best model from Step 2 to examine simple associations of baseline MRI variables with cognitive intercepts and slopes adjusted for covariates. These volumes included ICV, hippocampus (adjusted for ICV), total WMH, brain bl (the global baseline volume factor), and each lobar ROI adjusted for ICV—but not for brain bl. We then fitted four separate models that jointly included brain bl and ICV as well as each individual, specific lobar measurement as presented in Figure 1. Finally, we generated a multivariate model that jointly included

significant MRI variables from previous steps. We then followed a similar process for MRI change variables. We first examined simple associations with cognition, adjusted for covariates, then examined each lobe specific residual entered jointly with brain ch, and finally, fitted a multivariate model incorporating significant effects from previous analyses in this step.

In Step 4 we generated a final multivariable model that jointly included significant effects from previous steps. We then added to the Step 4 model to incorporate other variables that might influence cognitive decline, specifically vascular risk factors. Finally, we added parameters to estimate the associations of cognitive intercepts with brain change variables.

All parameters were simultaneously estimated within each model. Latent variables for MRI variables, latent random effects for cognitive variables, and regressions of cognitive random effects on MRI variables and covariates were simultaneously estimated. Although we estimated intercept random effects and evaluated the effects of MRI variables on intercepts, the focus of this report is on cognitive change so intercept results are not reported.

Complete data was not available on all variables. The largest component of missing data was for longitudinal MRI scans, where 165 of the 460 participants did not have longitudinal scans. The full sample of 460 was used for the primary data analyses and the missing data analysis option of Mplus was used. This approach effectively used all available data to estimate cognitive trajectories and effects of baseline brain variables and covariates on those trajectories. This maximizes precision of estimation of cognitive intercept and slope parameters and statistical power for detecting baseline brain and covariate effects. Power for detecting brain change effects is lower because of the reduced sample size for the brain change variables. Mplus uses full information maximum likelihood estimation, which provides unbiased parameter estimates in the context of missing at random (Newman, 2003). Missing at random is satisfied when missingness can be explained by observed variables in the model. We performed secondary analyses to evaluate whether the missing longitudinal MRI data biased results. Specifically, one secondary model excluded those participants who did not have longitudinal scans. A second analysis modeled the effects of missing longitudinal scans on cognitive trajectories, and examined whether baseline brain variables could explain missing longitudinal scans.

Mixed model regression analyses are sensitive to assumptions of linearity, normality, and constant variance. These assumptions were examined using graphical and statistical diagnostics. Residuals and random effects were examined to assure that they were normally distributed, and plots of residuals against predicted values and effects were examined to verify that nonlinear trends in the data or nonconstant variances were not present. Additional diagnostics included evaluation of variance components related to random effects and within subject error variance to address adequacy of statistical estimation procedures associated with the random effects modeling.

Voxelwise analysis of longitudinal change—We performed voxel based analyses to characterize the associations of brain regions with cognitive change. Voxelwise log-Jacobian images in template space enable cross-sectional averaging and regression analysis of

longitudinal change, to identify patterns of atrophy and associations with cognition independent of prior hypotheses about locations where these might occur. In voxel-based regressions, the log-Jacobian change value at a voxel was an independent variable with covariates of age, gender, education and interscan interval between baseline and follow-up scans. Outcomes or dependent variables were cognitive baseline (intercept) and change (slope) measurements estimated as described above from the Step 1 unconditional model that included a global slope. We focused on global cognitive slope as the outcome of interest. Significance testing for regression coefficients of log-Jacobian predicting cognitive outcomes was performed by nonparametric superthreshold cluster testing (Nichols & Holmes, 2002) with 1000 iterations of random permutations. Clusters of a determined threshold with size in the top 5% of the distribution generated by these iterations were deemed significant. We selected a range of thresholds for the coefficient *t* values, generating significant contiguous clusters for each threshold. To generate images of average estimated change over equivalent intervals, we further scaled each subject log-Jacobian image in MDT space by 2/Δ where Δ is the interscan interval. These normalized log-Jacobians represented change of each subject over two years.

Results

Descriptive statistics for brain and baseline cognition variables are presented in Table 2. All brain variables differed significantly across diagnosis groups (*ps* < 0.001 except for baseline frontal: $F(2, 402) = 6.487$, $p = .002$, baseline occipital: $F(2, 402) = 5.138$, $p = .006$, and occipital change: $F(2, 291) = 3.414$, $p = .034$). All cognitive variables differed across groups (*ps* < 0.001).

Voxel-Based Analysis

For an overview of atrophy rates in our cohort, we generated average log-Jacobians after normalizing interscan intervals to two years (see Figure 3). Cortical GM atrophy rates of about 2% appear concentrated in temporal gray regions, the entorhinal area and the posterior cingulate. Noncortical atrophy of the same magnitude appears in the thalamus, along with the genu and splenium of the corpus callosum, whereas higher rates of around 3% are visible in other portions of the corpus callosum. We performed regression models using the non-normalized (raw) log-Jacobians as predictors of cognitive baseline and cognitive slope, controlling for age, gender, education and also interscan interval. The largest magnitude range of *t* values was for the log-Jacobian predictors of cognitive slope, up to $t = 13$. As described above, we used a global slope measure of cognitive change as the outcome of interest. Our results indicated very strong positive association of cognitive change (slope) with brain atrophy, that is, smaller magnitude negative slopes (less cognitive loss) were associated with less atrophy and greater magnitude negative slopes with more atrophy. We tested for significant clusters of *t* values for log-Jacobians in the models predicting cognitive slope as described previously, selecting a range of *t* thresholds from 7 to 13. The results are displayed in Figure 4. Large clusters appear throughout the temporal lobes, with other clusters having generally lower *t* values in the thalamus, corpus callosum and posterior cingulate. The clusters suggest a concentration of significant associations of brain change with cognitive change in the temporal lobes (extremely high *t* values up to 13) with lower *t*

values of significant associations (7 to 8) in the thalamus, corpus callosum and posterior cingulate. Outcomes of cognitive baseline had much smaller *t* value magnitudes, with the highest being for verbal memory (+7.8). We tested significant clusters for verbal memory and found few coherent clusters. Ranges of *t* values for the other cognitive measures (spatial, executive and semantic) associated with log-Jacobians were never greater than + 5 and we did not test these measures for significant clusters.

Model for Cognitive Intercepts and Slopes

Figure 5 shows individual cognitive trajectories for randomly selected study participants. There is considerable variability both in level (starting point) of trajectories and in individual slopes across assessments. There is also considerable assessment-to- assessment variability around linear trend lines. This is common in longitudinal cognitive assessments, and highlights limits of reliability of the cognitive assessments. Reliability estimates for the four cognitive outcomes (measured by the intraclass correlation across repeated measurements in the unconditional model) were: episodic memory − 0.74, semantic memory − 0.84, executive function − 0.77, spatial ability − 0.61. Table 3 shows fit indices for different models for explaining covariance of cognitive intercepts and slopes. The best fitting model by all three criteria had separate intercepts for the four cognitive outcomes, but a global slope factor that accounted for covariance among the four slope random effects. Correlations in the unconditional Step 1 model with separate intercepts and slopes ranged from 0.53 to 0.80 for intercepts. In contrast, correlations among slope random effects ranged from 0.87 to 0.96. These results suggest that intercepts, although correlated, are dissociable, but that slopes are very highly correlated and reflect a unidimensional decline process. Subsequent results utilize a global slope factor to characterize cognitive decline. There was statistically significant variability in this global cognitive slope factor (estimate = 0.885, $SE = 0.191$, $p = .001$), indicating that there are important individual differences in rate of cognitive decline that can be potentially be explained by brain variables and covariates. We emphasize the effects of brain variables on cognitive decline measured by this global slope factor. None of the covariate by ethnicity interaction effects on global slope were significant (p's > 0.15), and so, these interactions were not included in subsequent models.

Brain Volume Effects on Global Cognitive Change—Single Variable Models

Table 4 shows effects of brain baseline and change variables on global cognitive slope. These models included one brain variable at a time and covariates. All baseline GM volumes were associated with cognitive change except for occipital volume and intracranial volume. Global GM and temporal lobe GM had the strongest, and approximately equal, effects among baseline brain measures. GM volume change in all lobar ROIs was related to cognitive change, and again, global GM change and temporal lobe change had the strongest effects. The GM change effects were substantially stronger that corresponding effects of baseline brain variables. Figure 6 visually summarizes the significant effects in univariate models of each lobe's GM atrophy on cognitive slope, color coded for effect sizes as presented in Table 4.

Specific Brain Volume Effects on Global Cognitive Change

The next step of analysis examined specific effects of incremental differences in lobar GM ROIs beyond those associated with differences in the global GM. The primary independent variables in these analyses were the global GM volumes (baseline and change) and lobar ROIs residualized for the corresponding GM volume, with baseline volumes additionally residualized for ICV. Separate models were fitted for each baseline GM ROI and each GM change ROI. For baseline volumes, only the temporal lobe ROI had a significant effect on global cognitive change beyond that of global baseline volume and the associated general difference in lobar ROI (global gray baseline: estimate = 0.022, *SE* = 0.007, *p* = .001; specific temporal baseline: estimate = 0.022, *SE* = 0.007, *p* = .003). This means that *less* temporal lobe atrophy, in comparison with what would be expected on the basis of global atrophy, would have a positive impact on rate of cognitive decline, whereas *greater* temporal lobe atrophy than expected would increase cognitive decline. A similar pattern was found for specific lobar GM change effects, where Specific Temporal GM Change (estimate = 0.033, *SE* = 0.007, *p* = .001) incrementally contributed to cognitive change beyond the effects of global GM change (estimate = 0.058, *SE* = 0.009, *p* = .001).

Multivariable Model Including Baseline Brain Volumes and Brain Volume Change

The final analytic model included brain baseline and change variables that were significantly associated with global cognitive change in previous steps, along with covariates. Brain volumes included as independent variables in the analysis were: baseline global GM, specific temporal lobe GM, hippocampus, and white matter hyperintensity and global GM change and specific temporal lobe GM change.

Table 5 shows covariate effects from this model. The intercept term in Table 5 represents the average rate of cognitive change (about 0.10 *SD* per year) for the reference condition in this analysis, that is, a Caucasian female 70 years old with 12 years of education recruited from the community, APOE e4 negative, and with average values (for this sample) on all brain imaging variables included in this analysis. African Americans declined at a significantly slower rate in comparison to Caucasians, and clinic recruitment source and APOE e4 positivity were associated with faster rates of decline.

Table 6 presents brain imaging variable effects from the multivariable model. Global GM change had the strongest impact on cognitive decline; a one *SD* increase in rate of GM atrophy was associated with an annual increase in rate of cognitive decline of 0.057 *SD.* Temporal lobe GM change made an incremental contribution to cognitive decline beyond the general effects of global GM change and all the other variables in the model. Baseline hippocampus and white matter hyperintensity also were related to cognitive change conditional on all other variables in the model. In summary, these results show that GM atrophy is the strongest predictor of cognitive decline, and temporal lobe atrophy makes a strong contribution above and beyond the effects of global atrophy and its associated mean impact on the temporal lobe. Additionally, individuals with larger hippocampi at baseline decline slower, whereas those with more white matter hyperintensities decline faster.

Vascular risk factors (presence/absence of hypertension, hypercholesterolemia, and diabetes at the baseline evaluations) were added as independent variables to test whether these variables explain individual differences in cognitive intercepts and global cognitive slope. None of these variables were related to global cognitive slope (p's > 0.43, results not shown). Adding vascular risk factors to the model did not alter the associations of global GM change, specific temporal lobe GM change, hippocampal volume, and white matter hyperintensity volume with global cognitive change (not shown).

Finally, we examined whether cognitive intercepts were associated with brain change. When regression paths were added to the model to estimate the effects of the four cognitive intercepts on the two brain change variables, the episodic memory intercept was related to both global GM change (estimate = 0.499, $SE = 0.107$, $p = .001$) and specific temporal lobe GM change (estimate = 0.593, $SE = 0.123$, $p = .001$) independent of the effects of the other three cognitive intercepts. Semantic memory, executive function, and spatial intercepts were not independently related to brain change variables. Again, effects of brain variables on global cognitive change were substantially the same as in previous multivariable models (not shown).

Secondary Analyses

We estimated the final multivariable model in an analysis that excluded participants who did not have longitudinal scans. Results were essentially unchanged with respect both to the pattern of significant results and the regression coefficients that characterize the effects of brain variables on cognitive change. A second analysis added a term to the final multivariable model to code for effects of missing longitudinal scans on cognitive trajectories and brain variables. Baseline brain variables were related to missing longitudinal scans, with greater baseline brain volumes in those with longitudinal scans. Cognitive slopes and intercepts were minimally different in those with and without longitudinal scans and effects of brain variables on cognitive decline were unchanged from the primary analysis.

Discussion

We used multilevel latent variable modeling methods to measure individual differences in rate of cognitive decline and then examined how baseline brain measurements, TBM measurements of longitudinal brain atrophy rates, and covariates explained differences in cognitive decline. We found that decline across multiple cognitive domains was very highly correlated and that domain specific decline was not dissociable from global cognitive decline. This contrasted with dissociable domain specific measures of baseline cognition. Longitudinal brain atrophy had the strongest effects on cognitive decline. Global GM loss was the strongest single predictor of cognitive decline but specific temporal lobe GM atrophy also contributed incrementally to cognitive decline. The pattern of salient temporal lobe effects was largely confirmed by TBM voxelwise analyses, which showed extremely strong associations with cognitive decline of log-Jacobians measuring local atrophy rates in temporal lobe locations and less strong but still highly significant associations in the thalamus and posterior cingulate (Figures 3–4). Baseline hippocampal volume and WMH load also made independent contributions to explaining cognitive decline. Baseline lobar

GM volumes were related to cognitive decline in models that did not include brain change effects.

Our findings point to a hierarchy of brain effects on cognitive loss. Longitudinal GM atrophy was the strongest contributor to cognitive decline in this study, with both global GM atrophy and temporal lobe specific atrophy making contributions. These results confirm previous TBM studies (McDonald et al., 2012; Murphy et al., 2010) that demonstrated the importance of temporal lobe GM in early cognitive decline. The importance of brain change effects over baseline effects suggests that longitudinal brain change, that is, atrophy, is the brain "implementation" of cognitive decline. GM volume loss is a well-established component of AD and also has been shown to result from other diseases leading to cognitive decline and dementia, especially cerebrovascular disease (Jagust et al., 2008; Seshadri et al., 2004; Zheng et al., 2016).

The salience of specific temporal lobe GM loss observed in this study fit well with progression of AD related brain injury described by Braak and Braak (1991, 1996) and literature showing that cognitive loss accelerates when AD neurofibrillary tangle pathology spreads first to temporal lobe neocortex and then more broadly to association cortex throughout the brain. Although longitudinal brain atrophy resulting from AD depends strongly on specific brain dynamics of amyloid-β and the patterned propagation of tau (Price & Morris, 1999; Schöll et al., 2016), other disease processes, notably cerebrovascular disease, undoubtedly make incremental contributions to cortical GM loss.

The cohort in this study is very diverse along many dimensions, and is not a highly selected sample that excludes non-AD disease processes. Specifically, this cohort has been enriched for vascular risk factors (Hinton et al., 2010; Lee et al., 2010) and has relatively high overall prevalence of diabetes, hypertension, and hypercholesterolemia. The salience for cognitive decline of temporal lobe GM atrophy, the VBM finding that posterior cingulate atrophy is strongly associated with cognitive decline, and the association of baseline hippocampal volume with cognitive decline suggest plausible mechanisms for AD contributions to cognitive decline; however, it is important to note that these changes may not be entirely specific to AD. The independent contribution of WMH to cognitive decline might point to an underlying vascular mechanism. WMH is widely regarded as an indicator of microvascular disease and is a well-established late life effect of midlife hypertension (Yoshita et al., 2006). However, WMH also is associated with AD (Kandel et al., 2016), and specifically, posterior WMH is influenced by AD whereas anterior WMH is more specific to cerebrovascular disease (Yoshita et al., 2006). We used a global measure of WMH in this study that did not separately examine posterior versus anterior WMH effects. This would be important to address in future studies. Nevertheless, the finding that WMH contributed to cognitive decline independently of multiple brain variables that are highly associated with AD provides evidence of a non-AD contribution to cognitive decline, which in the case of WMH, most likely reflects vascular disease. The independent contributions of baseline hippocampus and WMH effects on cognitive decline are consistent with the notion of a synergy of vascular and AD- pathology influences on early cognitive decline, as has been reported elsewhere (Brickman, 2013; Kandel et al., 2016; Scott et al., 2015).

To place our current results within the context of the views emerging from recent studies, we concur on the primary effects of whole brain atrophy rates (Sluimer et al., 2010) and temporal lobe GM atrophy (McDonald et al., 2012; Mungas et al., 2005a; Murphy et al., 2010; Rodrigue & Raz, 2004) for cognitive change. Our finding of the primacy of temporal lobe atrophy also concurs with patterns of normal aging or among those with very low risk of AD (Fjell et al., 2013; Fjell et al., 2009). This may lend weight to the hypothesis that pathways of normal and disease based cognitive aging correspond to similar atrophy patterns in the brain but are exaggerated in the presence of disease.

Our study also shows some differences with previous results. For example, in a longitudinal study from our group using a different sample, brain effects on cognitive decline differed by domain (Mungas et al., 2005a). In that study, change in memory was primarily related to hippocampus baseline and change and executive function decline was more broadly related to cortical GM atrophy, WMH, and hippocampal atrophy. Our current study included a larger number of cognitive domains, and decline across these domains was highly correlated and consequently not separable in analytic models. This finding suggests that aging and age-related diseases have general, multidomain effects on cognitive decline. Because of such global effects, we did not examine differential brain effects on domain specific cognitive change in this study. This is not to say that global decline is the general rule. The sample in this study was not well represented by diseases that might generate greater cross-domain heterogeneity in cognitive decline, for example, focal cortical stroke or focal manifestations of frontal temporal degeneration. With respect to this specific cohort, previous studies have shown that episodic memory is the most sensitive indicator of cognitive decline, whereas semantic memory provides the most reliable measure of cognitive decline (Mungas et al., 2010). Results of the current study show that cognitive decline is highly correlated across cognitive domains and that this cognitive change is best explained by GM atrophy. Future studies are needed to better address determinants of domain specific cognitive decline.

These findings have clinical implications. The results presented in Table 3 show that individual cognitive domains are dissociable at baseline, but change in concert with one another such that a global slope fit the data better than domain specific slopes. Baseline cognitive test scores are strongly influenced by life experiences (Melrose et al., 2015). Therefore, differential diagnosis among competing dementia etiologies would likely benefit from interpretation of cross-sectional test score patterns while accounting for relevant between group differences (e.g., race/ethnicity) and important life experience variables such as education (Early et al., 2013). In contrast, changes in cognition are important for monitoring disease progression, but perhaps less valuable for differentiating underlying etiologies. These results also suggest that cross-sectional GM volume is useful for predicting future rate of cognitive decline, but does not add to explaining cognitive decline when brain change measures are available. With the exception of baseline hippocampus volume and WMH, cognitive decline is largely governed by GM atrophy, which is common in nearly all neurodegenerative conditions. Finally, our results show the baseline episodic memory was a particularly strong predictor of future brain atrophy, and this supports the notion that memory impairment in a cross-sectional assessment has utility for predicting future rate of brain disease progression.

We did not find that common vascular risk factors were associated with cognitive decline, nor were associations of brain variables with cognitive decline different when effects of vascular risk factors were included in the analytic model. Further research is needed to better understand the role of vascular risk factors. There is clear evidence that life course exposure to vascular risk factors is associated with late life brain variables and that cognition is inversely related to vascular disease (Seshadri et al., 2004; Zheng et al., 2012). A conceptual model in which vascular risk exposure leads to vascular brain injury that is one of potentially many causes of cognitive decline seems reasonable, and future studies can help to explicitly and systematically test these pathways to cognitive decline.

This study has several limitations. First, in the interest of constructing manageable statistical models, we limited our choice of brain regions to lobar GM ROIs. This has enabled us to perform a sequence of tests leading to a very clear hierarchy of brain effects on cognition. However, as many studies have shown, TBM is capable of fine-grained spatial resolution. This suggests that a valuable future agenda would be to attempt a similar analysis focusing on white matter tracts and GM regions known to be preferentially vulnerable to Alzheimer's pathology, for example the GM nodes and white matter connections of the default mode network (Greicius, Srivastava, Reiss, & Menon, 2004) or limbic circuit (Nestor, Fryer, Smielewski, & Hodges, 2003). Second, we have reported effects of brain measurements on cognitive change without regard to ethno-racial category. Race and ethnicity may be important proxies for variables that influence brain changes, with the important consequence that "typical" scenarios of dementia trajectories in Caucasian populations may not be applicable to diverse populations with different mixes of risk factors (genetic, cardiovascular and metabolic). This question is being addressed in a companion paper that examines similarities and differences of brain-cognition relations across racial-ethnic groups. A third limitation relates to the time frame over which we have captured cognitive and brain measurements in our data set. Our baseline measurements are a current-time snapshot which are in turn outcomes of factors earlier in life to which we do not have access. Future decades-long data sets, ideally beginning in presymptomatic young subjects (e.g., Reiman et al., 2011) may well elucidate further the relative contributions of longitudinal brain change to cognitive trajectories.

Another important limitation of this study and related research is that results are essentially correlational and this presents limitations for making causal inferences. The longitudinal design of this study does add to the potential for causal inference. Specifically, our ability to estimate associations of baseline brain variables and change in brain variables with longitudinal change in cognition strengthens causal inferences regarding brain mechanisms of cognitive decline (Salthouse, 2011). Although it seems reasonable based on a priori theory to infer that brain changes result in cognitive decline, this process is complex and not fully explainable within the context of this study. The associations of baseline episodic memory with global and temporal lobe GM changes exemplify this complexity. It is theoretically unlikely that cognition causes brain change and a more reasonable explanation is that episodic memory is an indicator for a disease process that is causing both cognitive decline and brain atrophy. Our study did not include direct measures of underlying disease processes, for example, biomarkers for AD, and this limits our ability to fully characterize the causal paths leading to cognitive decline.

This study also has important strengths. It combined comprehensive assessment of cognition using psychometrically sophisticated and matched outcome measures with comprehensive measurement of baseline brain status and brain change in a longitudinal cohort that now has been followed over a substantial amount of time. The sample in this study was very heterogeneous, not only in racial and ethnic characteristics, but also in variability of the TBM and cognitive measures. As such, the results can be generalized across a broad spectrum of brain integrity and dementia severity, including those without brain pathology or cognitive impairment.

The question of what is healthy cognitive aging that is not attributable to age related disease has been a central and difficult to resolve issue in cognitive aging research. Defining what is healthy aging is central to answering this question, but this is especially challenging given that AD and CVD pathologies are commonly observed in cognitively normal individuals (Davis, Schmitt, Wekstein, & Markesbery, 1999; Fjell et al., 2013; Fjell et al., 2014; Soderlund, Nyberg, Adolfsson, Nilsson, & Launer, 2003). Sensitive measurement of brain variables and change in brain variables across a broad spectrum of brain health and disease adds potentially valuable information that might help to define and quantify brain disease. Results of this study showed that cognitive decline is strongly related to brain change. Previous work with this cohort showed that cognitive decline also is strongly associated with independently established change in clinical diagnosis (Mun- gas et al., 2010). In this study we observed clear differences in brain variables across diagnostic groups (see Table 2). These results converge to suggest that cognitive decline results from clinically relevant manifestations of brain changes. The question of whether these brain changes are at least partly due to “normal” aging cannot be definitively addressed in this study because we do not have direct measures/biomarkers of the many diseases that could influence the brain changes that we observed in this sample. But we can clearly say that individuals with stable brain measures across time are at substantially decreased risk for cognitive decline and presumably clinical progression and increasing disability. Further research that incorporates additional disease biomarkers with imaging measures of brain changes will help to differentiate healthy and pathological cognitive aging.

References

Akaike H (1987). Factor analysis and AIC. Psychometrika, 52, 317–332. 10.1007/BF02294359

Aljabar P, Heckemann RA, Hammers A, Hajnal JV, & Rueckert D (2009). Multi-atlas based segmentation of brain images: Atlas selection and its effect on accuracy. NeuroImage, 46, 726–738. 10.1016/j.neuroimage.2009.02.018 [PubMed: 19245840]

Ashburner J, & Friston KJ (2000). Voxel-based morphometry-the methods. Neuroimage, 11, 805–821. 10.1006/nimg.2000.0582 [PubMed: 10860804]

Braak H, & Braak E (1991). Neuropathological staging of Alzheimer-related changes. Acta Neuropathologica, 82, 239–259. [PubMed: 1759558]

Braak H, & Braak E (1996). Evolution of the neuropathology of Alzheimer’s disease. Acta Neurologica Scandinavica, 94, 3–12. 10.1111/j.1600-0404.1996.tb05866.x

Brickman AM (2013). Contemplating Alzheimer’s disease and the contribution of white matter hyperintensities. Current Neurology and Neuroscience Reports, 13 10.1007/s11910-013-0415-7

Christensen GE, Joshi SC, & Miller MI (1997). Volumetric transformation of brain anatomy IEEE Transactions on Medical Imaging, 16, 864–877. 10.1109/42.650882 [PubMed: 9533586]

Crane PK, Narasimhalu K, Gibbons LE, Pedraza O, Mehta KM, Tang Y, … Mungas DM (2008). Composite scores for executive function items: Demographic heterogeneity and relationships with quantitative magnetic resonance imaging. Journal of the International Neuropsychological Society, 14, 746–759. 10.1017/S1355617708081162 [PubMed: 18764970]

Davatzikos C, Genc A, Xu D, & Resnick SM (2001). Voxel-based morphometry using the RAVENS maps: Methods and validation using simulated longitudinal atrophy. Neuroimage, 14, 1361–1369. 10.1006/nimg.2001.0937 [PubMed: 11707092]

Davis DG, Schmitt FA, Wekstein DR, & Markesbery WR (1999). Alzheimer neuropathologic alterations in aged cognitively normal subjects. Journal of Neuropathology and Experimental Neurology, 58, 376–388. [PubMed: 10218633]

Driscoll I, Davatzikos C, An Y, Wu X, Shen D, Kraut M, & Resnick SM (2009). Longitudinal pattern of regional brain volume change differentiates normal aging from MCI. Neurology, 72, 1906–1913. 10.1212/WNL.0b013e3181a82634 [PubMed: 19487648]

Early DR, Widaman KF, Harvey D, Beckett L, Park LQ, Farias ST, … Mungas D (2013). Demographic predictors of cognitive change in ethnically diverse older persons. Psychology and Aging, 28, 633–645. 10.1037/a0031645 [PubMed: 23437898]

Fjell AM, McEvoy L, Holland D, Dale AM, & Walhovd KB (2013). Brain changes in older adults at very low risk for Alzheimer's disease. The Journal of Neuroscience, 33, 8237–8242. 10.1523/JNEUROSCI.5506-12.2013 [PubMed: 23658162]

Fjell AM, McEvoy L, Holland D, Dale AM, & Walhovd KB (2014). What is normal in normal aging? Effects of aging, amyloid and Alzheimer's disease on the cerebral cortex and the hippocampus. Progress in Neurobiology, 117, 20–40. 10.1016/j.pneurobio.2014.02.004 [PubMed: 24548606]

Fjell A, Walhovd KB, Fennema-Notestine C, McEvoy LK, Hagler DJ, Holland D, … Dale AM (2009). One-year brain atrophy evident in healthy aging. The Journal of Neuroscience, 29, 15223–15231. 10.1523/JNEUROSCI.3252-09.2009 [PubMed: 19955375]

Fletcher E (2014). Using prior information to enhance sensitivity of longitudinal brain change computation In Chen CH (Ed.), Frontiers of medical imaging (pp. 63–81). Hackensack, NJ: World Scientific 10.1142/9789814611107_0004

Fletcher E, Knaack A, Singh B, Lloyd E, Wu E, Carmichael O, & DeCarli C (2013). Combining boundary-based methods with tensor-based morphometry in the measurement of longitudinal brain change. IEEE Transactions on Medical Imaging, 32, 223–236. 10.1109/tmi.2012.2220153 [PubMed: 23014714]

Fletcher E, Singh B, Harvey D, Carmichael O, & DeCarli C (2012). Adaptive image segmentation for robust measurement of longitudinal brain tissue change. Conference Proceedings of IEEE in Engineering and Medicine and Biology Society, 2012, 5319–5322. 10.1109/EMBC.2012.6347195

Fletcher E, Villeneuve S, Maillard P, Harvey D, Reed B, Jagust W, & Decarli C (2016). Beta-amyloid, hippocampal atrophy and their relation to longitudinal brain change in cognitively normal individuals. Neurobiology of Aging, 40, 173–180. 10.1016/j.neurobiolaging.2016.01.133 [PubMed: 26973117]

Greicius MD, Srivastava G, Reiss AL, & Menon V (2004). Default-mode network activity distinguishes Alzheimer's disease from healthy aging: Evidence from functional MRI. Proceedings of the National Academy of Sciences, 101, 4637–4642. 10.1073/pnas.0308627101

Hinton L, Carter K, Reed BR, Beckett L, Lara E, DeCarli C, & Mungas D (2010). Recruitment of a community-based cohort for research on diversity and risk of dementia. Alzheimer Disease and Associated Disorders, 24, 234–241. 10.1097/WAD.0b013e3181c1ee01 [PubMed: 20625273]

Holland D, & Dale AM (2011). Nonlinear registration of longitudinal images and measurement of change in regions of interest. Medical Image Analysis, 15, 489–497. 10.1016/j.media.2011.02.005 [PubMed: 21388857]

Jagust WJ, Zheng L, Harvey DJ, Mack WJ, Vinters HV, Weiner MW, … Chui HC (2008). Neuropathological basis of magnetic resonance images in aging and dementia. Annals of Neurology, 63, 72–80. [PubMed: 18157909]

Kandel BM, Avants BB, Gee JC, McMillan CT, Erus G, Doshi J, … Wolk DA (2016). White matter hyperintensities are more highly associated with preclinical Alzheimer's disease than imaging and

cognitive markers of neurodegeneration. Alzheimer's & Dementia: Diagnosis, Assessment & Disease Monitoring, 4, 18–27. 10.1016/j.dadm.2016.03.001

Kochunov P, Lancaster JL, Thompson P, Woods R, Mazziotta J, Hardies J, & Fox P (2001). Regional spatial normalization: Toward an optimal target Journal of Computer Assisted Tomography, 25, 805–816. 10.1097/00004728-200109000-00023 [PubMed: 11584245]

Lee DY, Fletcher E, Martinez O, Zozulya N, Kim J, Tran J, … DeCarli C (2010). Vascular and degenerative processes differentially affect regional interhemispheric connections in normal aging, mild cognitive impairment, and Alzheimer disease. Stroke, 41, 1791–1797. 10.1161/STROKEAHA.110.582163 [PubMed: 20595668]

Leow AD, Yanovsky I, Chiang MC, Lee AD, Klunder AD, Lu A, … Thompson PM (2007). Statistical properties of Jacobian maps and the realization of unbiased large-deformation nonlinear image registration. IEEE Transactions on Medical imaging, 26, 822–832. 10.1109/TMI.2007.892646 [PubMed: 17679333]

McDonald CR, Gharapetian L, McEvoy LK, Fennema-Notestine C, Hagler DJ, Holland D, & Dale AM (2012). Relationship between regional atrophy rates and cognitive decline in mild cognitive impairment. Neurobiology of Aging, 33, 242–253. 10.1016/j.neurobiolaging.2010.03.015 [PubMed: 20471718]

Melrose RJ, Brewster P, Marquine MJ, MacKay-Brandt A, Reed B, Farias ST, & Mungas D (2015). Early life development in a multiethnic sample and the relation to late life cognition. Journals of Gerontology: Psychological Sciences and Social Sciences, 70B, 519–531. 10.1093/geronb/gbt126

Mungas D, Beckett L, Harvey D, Farias ST, Reed B, Carmichael O, … DeCarli C (2010). Heterogeneity of cognitive trajectories in diverse older persons. Psychology and Aging, 25, 606–619. 10.1037/a0019502 [PubMed: 20677882]

Mungas D, Harvey D, Reed BR, Jagust WJ, DeCarli C, Beckett L, … Chui HC (2005a). Longitudinal volumetric MRI change and rate of cognitive decline. Neurology, 65, 565–571. [PubMed: 16116117]

Mungas D, Reed BR, Crane PK, Haan MN, & González H (2004). Spanish and English Neuropsychological Assessment Scales (SENAS): Further development and psychometric characteristics Psychological Assessment, 16, 347–359. 10.1037/1040-3590.16.4.347 [PubMed: 15584794]

Mungas D, Reed BR, Haan MN, & Gonzalez H (2005b). Spanish and English Neuropsychological Assessment Scales: Relationship to demographics, language, cognition, and independent function. Neuropsychology, 19, 466–475. [PubMed: 16060821]

Mungas D, Reed BR, Marshall SC, & González HM (2000). Development of psychometrically matched English and Spanish language neuropsychological tests for older persons. Neuropsychology, 14, 209–223. 10.1037/0894-4105.14.2.209 [PubMed: 10791861]

Mungas D, Reed BR, Tomaszewski Farias S, & DeCarli C (2005). Criterion-referenced validity of a neuropsychological test battery: Equivalent performance in elderly Hispanics and non-Hispanic Whites. Journal of the International Neuropsychological Society, 11, 620–630. 10.1017/S1355617705050745 [PubMed: 16212690]

Mungas D, Widaman KF, Reed BR, & Tomaszewski Farias S (2011). Measurement invariance of neuropsychological tests in diverse older persons. Neuropsychology, 25, 260–269. 10.1037/a0021090 [PubMed: 21381830]

Murphy EA, Holland D, Donohue M, McEvoy LK, Hagler DJ, Dale AM, & Brewer JB (2010). Six-month atrophy in MTL structures is associated with subsequent memory decline in elderly controls. Neuroimage, 53, 1310–1317. 10.1016/j.neuroimage.2010.07.016 [PubMed: 20633660]

Muthén L, & Muthén B (1998–2012). Mplus user's guidebook (7th ed.). Los Angeles, CA: Author.

Nestor PJ, Fryer TD, Smielewski P, & Hodges JR (2003). Limbic hypometabolism in Alzheimer's disease and mild cognitive impairment. Annals of Neurology, 54, 343–351. 10.1002/ana.10669 [PubMed: 12953266]

Newman DA (2003). Longitudinal modeling with randomly and systematically missing data: A simulation of ad hoc, maximum likelihood, and multiple imputation techniques. Organizational Research Methods, 6, 328–362.

Nichols TE, & Holmes AP (2002). Nonparametric permutation tests for functional neuroimaging: A primer with examples. Human Brain Mapping, 15, 1–25. 10.1002/hbm.1058 [PubMed: 11747097]

Pini L, Pievani M, Bocchetta M, Altomare D, Bosco P, Cavedo E, … Frisoni GB (2016). Brain atrophy in Alzheimer's disease and aging. Ageing Research Reviews, 1–24. 10.1016/j.arr.2016.01.002

Price JL, & Morris JC (1999). Tangles and plaques in nondemented aging and "preclinical" Alzheimer's disease. Annals of Neurology, 45, 358–368. [PubMed: 10072051]

Raz N, Gunning FM, Head D, Dupuis JH, McQuain J, Briggs SD, … Acker JD (1997). Selective aging of the human cerebral cortex observed in vivo: Differential vulnerability of the prefrontal gray matter. Cerebral Cortex, 7, 268–282. [PubMed: 9143446]

Raz N, Lindenberger U, Rodrigue KM, Kennedy KM, Head D, Williamson A, … Acker JD (2005). Regional brain changes in aging healthy adults: General trends, individual differences and modifiers. Cerebral Cortex, 15, 1676–1689. 10.1093/cercor/bhi044 [PubMed: 15703252]

Raz N, & Rodrigue KM (2006). Differential aging of the brain: Patterns, cognitive correlates and modifiers. Neuroscience and Biobehavioral Reviews, 30, 730–748. 10.1016/j.neubiorev.2006.07.001 [PubMed: 16919333]

Reiman EM, Langbaum JB, Fleisher AS, Caselli RJ, Chen K, Ayutyanont N, … Tariot PN (2011). Alzheimer's prevention initiative: A plan to accelerate the evaluation of presymptomatic treatments. Journal of Alzheimer's Disease, 26, 321–329. 10.3233/JAD-2011-0059

Resnick SM, Pham DL, Kraut MA, Zonderman AB, & Davatzikos C (2003). Longitudinal magnetic resonance imaging studies of older adults: A shrinking brain. Journal of Neuroscience, 23, 3295–3301. [PubMed: 12716936]

Rodrigue KM, & Raz N (2004). Shrinkage of the entorhinal cortex over five years predicts memory performance in healthy adults. Journal of Neuroscience, 24, 956–963. 10.1523/JNEUROSCI.4166-03.2004 [PubMed: 14749440]

Rueckert D, Aljabar P, Heckemann RA, Hajnal JV, & Hammers A (2006). Diffeomorphic registration using B-splines In Larsen R, Nielsen M, & Sporring J (Eds.), MICCAI Conference Proceedings (Vol. 4191, pp. 702–709). New York, NY: Springer-Verlag.

Salthouse TA (2011). Neuroanatomical substrates of age-related cognitive decline. Psychological Bulletin, 137, 753–784. 10.1037/a0023262 [PubMed: 21463028]

Scholl M, Lockhart SN, Schonhaut DR, Schwimmer HD, Rabinovici GD, Correspondence WJJ, … Jagust WJ (2016). PET imaging of tau deposition in the aging human brain. Neuron, 89, 971–982. 10.1016/j.neuron.2016.01.028 [PubMed: 26938442]

Schwarz G (1978). Estimating the dimension of a model Annals of Statistics, 6, 461–464. 10.1214/aos/1176344136

Sclove SL (1987). Application of model-selection criteria to some problems in multivariate analysis Psychometrika, 52, 333–343. 10.1007/BF02294360

Scott JA, Braskie MN, Tosun D, Thompson PM, Weiner M, DeCarli C, & Carmichael OT (2015). Cerebral amyloid and hypertension are independently associated with white matter lesions in elderly. Frontiers in Aging Neuroscience, 7, 1–9. 10.3389/fnagi.2015.00221 [PubMed: 25653617]

Seshadri S, Wolf PA, Beiser A, Elias MF, Au R, Kase CS, … DeCarli C (2004). Stroke risk profile, brain volume, and cognitive function: The Framingham Offspring Study. Neurology, 63, 1591–1599. [PubMed: 15534241]

Sluimer JD, Bouwman FH, Vrenken H, Blankenstein MA, Barkhof F, Flier WM van der, & Scheltens P (2010). Whole-brain atrophy rate and CSF biomarker levels in mci and ad: A longitudinal study. Neurobiology of Aging, 31, 758–764. 10.1016/j.neurobiolaging.2008.06.016 [PubMed: 18692273]

Soderlund H, Nyberg L, Adolfsson R, Nilsson LG, & Launer LJ (2003). High prevalence of white matter hyperintensities in normal aging: Relation to blood pressure and cognition. Cortex, 39, 1093–1105. [PubMed: 14584568]

Yanovsky I, Leow AD, Lee S, Osher SJ, & Thompson PM (2009). Comparing registration methods for mapping brain change using tensor-based morphometry. Medical Image Analysis, 13, 679–700. 10.1016/j.media.2009.06.002 [PubMed: 19631572]

Yoshita M, Fletcher E, Harvey D, Ortega M, Martinez O, Mungas DM, … DeCarli CS (2006). Extent and distribution of white matter hyperintensities in normal aging, MCI, and ad. Neurology, 67, 2192–2198. 10.1212/01.wnl.0000249119.95747.1f [PubMed: 17190943]

Zheng L, Mack WJ, Chui HC, Heflin L, Mungas D, Reed B, … Kramer JH (2012). Coronary artery disease is associated with cognitive decline independent of changes on magnetic resonance imaging in cognitively normal elderly adults. Journal of the American Geriatrics Society, 60, 499–504. 10.1111/j.1532-5415.2011.03839.x [PubMed: 22283410]

Zheng L, Vinters HV, Mack WJ, Weiner MW, Chui HC, & project, I. V. D. program. (2016). Differential effects of ischemic vascular disease and Alzheimer's disease on brain atrophy and cognition. Journal of Cerebral Blood Flow and Metabolism, 36, 204–215. 10.1038/jcbfm.2015.152 [PubMed: 26126864]

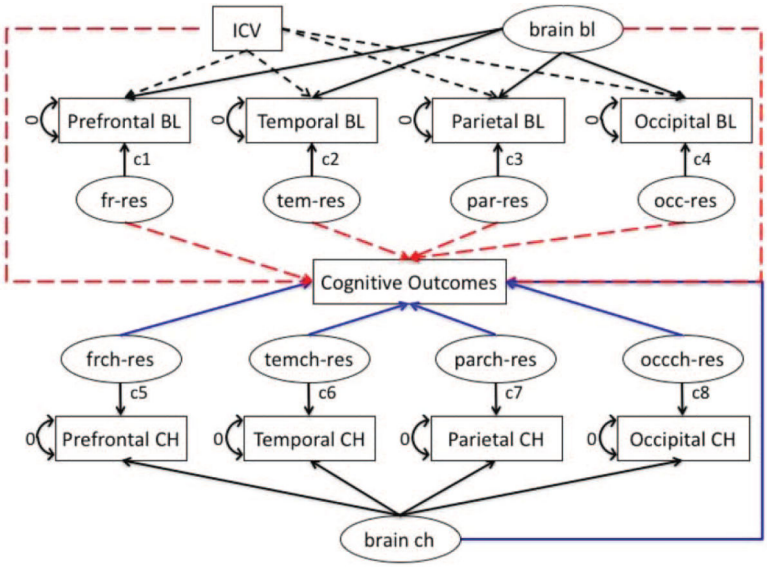

Figure 1.

Analytic model for decomposing MRI baseline and change. See the online article for the color version of this figure.

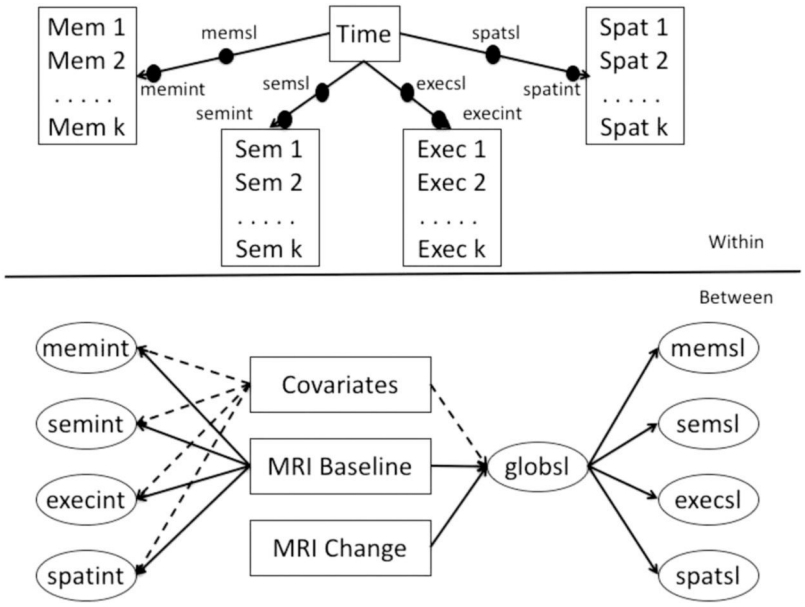

Figure 2.
Analytic model for cognitive trajectory components, MRI variables, and covariates.

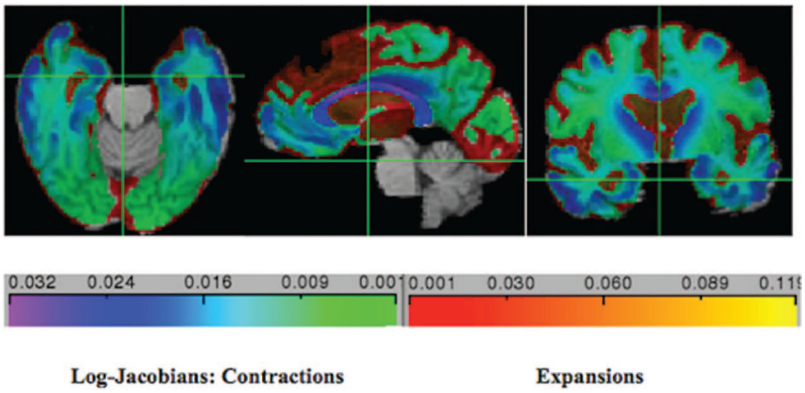

Figure 3.

Average 2-year losses for the study cohort. Grayscale bars (color online: cool palette left, warm palette right) show rates of contraction (cool palette left) or expansion (warm palette right) in this period. Log-Jacobian values are roughly equal to percentage changes. See the online article for the color version of this figure.

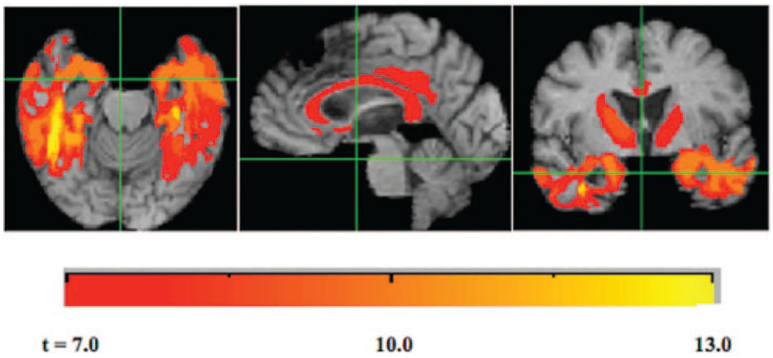

Figure 4.

Clusters of significant association for log-Jacobian brain change predicting global cognitive slope as outcome, controlling for age, gender and education. Grayscale bar indicates *t* threshold levels for clusters. Clusters are significant by size 1,000-iteration correction for multiple comparisons. See the online article for the color version of this figure.

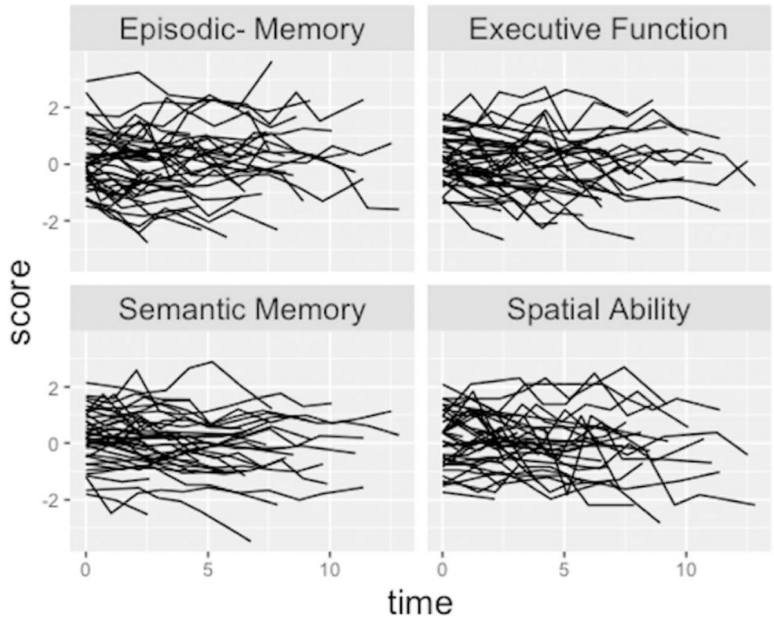

Figure 5.
Individual cognitive trajectories of 40 randomly selected participants.

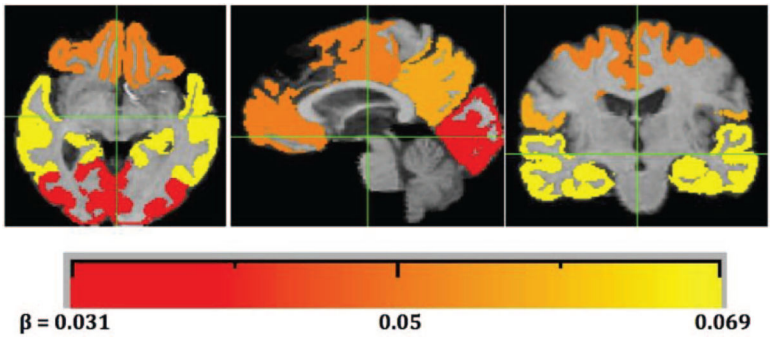

Figure 6.

Lobar regions color coded by effect sizes of univariate association of ROI atrophy with cognitive slope (see Table 3). Grayscale bar (color in online edition) indicates the effect size estimate in Table 3 for atrophy over each lobar region. Smallest effect size is for occipital (dark gray for print, red for online editions). Intermediate are prefrontal and parietal (darker and lighter shades of gray (print) or orange (color), respectively) and highest is temporal (yellow). See the online article for the color version of this figure.

Table 1

Sample Characteristics—Clinical and Demographic

Category	Demented	MCI	Normal	Total
Gender—Female	33 (57.9%)	82 (49.4%)	153 (66.2%)	268 (59.0%)
Gender—Male	24 (42.1%)	84 (50.6%)	78 (33.8%)	186 (41.0%)
Age—M (SD)	77.5 (±7.0)	75.0 (±7.0)	73.4 (±6.7)	74.5 (±7.0)
Education—M (SD)	11.5 (±4.7)	13.8 (±4.4)	12.8 (±4.4)	13.0 (±4.5)
Recruitment source—Clinic	28 (49.1%)	85 (51.2%)	32 (13.9%)	145 (31.9%)
Recruitment source—Community	29 (50.9%)	81 (48.8%)	199 (86.1%)	309 (68.1%)
Race/ethnicity—African American	15 (26.3%)	37 (22.3%)	68 (29.4%)	120 (26.4%)
Race/ethnicity—Hispanic	19 (33.3%)	17 (10.2%)	72 (31.2%)	108 (23.8%)
Race/ethnicity—Other	0 (0.0%)	7 (4.2%)	9 (3.9%)	16 (3.5%)
Race/ethnicity—White	23 (40.4%)	105 (63.3%)	82 (35.5%)	210 (46.3%)
APOE e4–0	22 (38.6%)	88 (53.0%)	161 (69.7%)	271 (59.7%)
APOE e4–1	35 (61.4%)	78 (47.0%)	70 (30.3%)	183 (40.3%)
Hypertension (baseline)—Absent	19 (35.2%)	60 (38.0%)	68 (30.9%)	147 (34.0%)
Hypertension (baseline)—Present	35 (64.8%)	98 (62.0%)	152 (69.1%)	285 (66.0%)
Hypercholesterolemia (baseline)—Absent	26 (50.0%)	75 (46.9%)	99 (47.1%)	200 (47.4%)
Hypercholesterolemia (baseline)—Present	26 (50.0%)	85 (53.1%)	111 (52.9%)	222 (52.6%)
Diabetes (baseline)—Absent	44 (81.5%)	124 (77.0%)	145 (65.9%)	313 (72.0%)
Diabetes (baseline)—Present	10 (18.5%)	37 (23.0%)	75 (34.1%)	122 (28.0%)

Note. N = 460. Diagnosis was missing for 6 individual; hypertension, for 22; hypercholesterolemia, for 32; diabetes, for 19. MCI = mild cognitively impaired; APOE = apolipoprotein E.

Table 2

Sample Characteristics—Baseline Brain and Cognition, and Change in Lobar Cortical Gray

Brain/cognition category	Demented	MCI	Normal	Total
Prefrontal gray BL[a]—*M* (SD)	−3.3 (±8.7)	−0.6 (±8.1)	1.2 (±8.1)	0.0 (±8.3)
Prefrontal gray BL[a]—Missing	8 (14.0%)	21 (12.7%)	20 (8.7%)	49 (10.8%)
Temporal gray BL[a]—*M* (*SD*)	−9.6 (±10.5)	−2.0 (±9.2)	3.7 (±7.1)	0.1 (±9.4)
Temporal gray BL[a]—Missing	8 (14.0%)	21 (12.7%)	20 (8.7%)	49 (10.8%)
Parietal gray BL[ac]—*M* (*SD*)	−2.8 (±5.1)	−0.7 (±5.7)	1.2 (±4.9)	0.0 (±5.4)
Parietal gray BL[ac]—Missing	8 (14.0%)	21 (12.7%)	20 (8.7%)	49 (10.8%)
Occipital gray BL[a]—*M (SD)*	−1.1 (±5.3)	−0.8 (±6.5)	0.9 (±4.8)	0.0 (±5.6)
Occipital gray BL[a]—Missing	8 (14.0%)	21 (12.7%)	20 (8.7%)	49 (10.8%)
Hippocampus BL[a]—*M* (SD))	−0.8 (±0.7)	−0.2 (±0.7)	0.3 (±0.6)	0.0 (±0.8)
Hippocampus BL[a]—Missing	9 (15.8%)	22 (13.3%)	25 (10.8%)	56 (12.3%)
White matter hyperintensity BL—*M* (*SD*)	17.0 (±17.8)	14.2 (±15.4)	10.1 (±11.8)	12.4 (±14.2)
White matter hyperintensity BL—Missing	8 (14.0%)	21 (12.7%)	20 (8.7%)	49 (10.8%)
Prefrontal gray change[b]—*M* (*SD*)	−1.4 (±.7)	−1.2 (±0.9)	−0.8 (±0.5)	−1.0 (±0.7)
Temporal gray change[b]—*M* (*SD*)	−1.9 (±1.0)	−1.3 (±1.0)	−0.7 (±0.5)	−1.0 (±0.8)
Parietal gray change[bc]—*M* (*SD*)	−1.4 (±1.1)	−1.1 (±0.8)	−0.7 (±0.5)	−0.9 (±0.7)
Occipital gray change[b]—*M* (*SD*)	−0.5 (±.8)	−0.5 (±0.7)	−0.3 (±0.6)	−0.4 (±0.6)
Episodic memory BL—*M* (*SD*)	−1.0 (±.5)	−0.4 (±0.7)	0.5 (±0.8)	−0.0 (±0.9)
Semantic memory BL—*M (SD)*	−0.8 (±1.0)	0.0 (±0.8)	0.2 (±0.9)	0.0 (±0.9)
Executive function BL—*M* (*SD*)	−0.7 (±0.9)	−0.1 (±0.7)	0.4 (±0.9)	0.1 (±0.9)
Spatial BL—*M (SD)*	−0.6 (±1.0)	−0.1 (±0.9)	0.2 (±0.9)	0.0 (±1.0)

Note. BL = baseline.

[a]Residualiized for intracranial volume.

[b]Log Jacobian × 100.

[c] Minus postcentral gyrus.

Table 3

Fit Indices of Alternate Models to Characterized Covariance Among Cognitive Intercepts. Slopes Best Fit Indices of Each Model are Indicated in Bold

Model	AIC	BIC	aBIC
Separate intercepts—Separate slopes	16,562	16,925	16,728
Global intercept—Separate slopes	16,696	16,978	16,825
Separate intercepts—Global slope	16,560	16,842	16,689
Global intercept—Global slope	16,696	16,930	16,803

Table 4

Baseline Brain Volume and Brain Volume Change Effects on Global Cognitive Change—Univariable Models

Variable	Estimate	*SE*	*p*
Global gray baseline	.03	.007	.001
Prefrontal gray baseline	.019	.006	.001
Temporal gray baseline	.032	.006	.001
Parietal gray baseline	.017	.006	.003
Occipital gray baseline	.004	.005	.486
Hippocampus baseline	.036	.006	.001
White matter hyperintensity baseline	-.019	.005	.001
Intracranial volume baseline	-.005	.008	.48
Global gray change	.061	.009	.001
Prefrontal gray change	.051	.008	.001
Temporal gray change	.069	.009	.001
Parietal gray change	.058	.009	.001
Occipital gray change	.031	.008	.001

Note. These results are from models that included one brain variable at a time along with covariates.

Table 5

Covariate Effects on Global Cognitive Change From Final Multivariable Model

Variable	Estimate	*SE*	*p*
Intercept (reference)	−.097	.014	.001
Male	.011	.012	.353
Education	.001	.001	.357
Spanish	−.021	.015	.168
African American	.038	.012	.001
Hispanic	.026	.014	.051
Other ethnicity	.011	.023	.629
Age (baseline)	.00	.001	.801
Clinic recruitment	−.054	.013	.001
APOE e4	−.032	.009	.001

Note. APOE = apolipoprotein E.

Table 6

Brain Volume Effects on Global Cognitive Change From Final Multivariable Model

Variable	Estimate	*SE*	*p*
Global gray BL	.001	.006	.859
Temporal gray BL	−.002	.007	.743
Hippocampus BL	.018	.006	.003
White matter hyperintensity BL	−.016	.005	.001
Global gray CH	.059	.01	.001
Temporal gray CH res	.029	.007	.001

Note. BL = baseline; CH = change.